Supplemental Information

Actin filament severing by cofilin dismantles actin patches and produces mother filaments for new patches

Qian Chen[1] and Thomas D. Pollard

Inventory of Supplemental Information

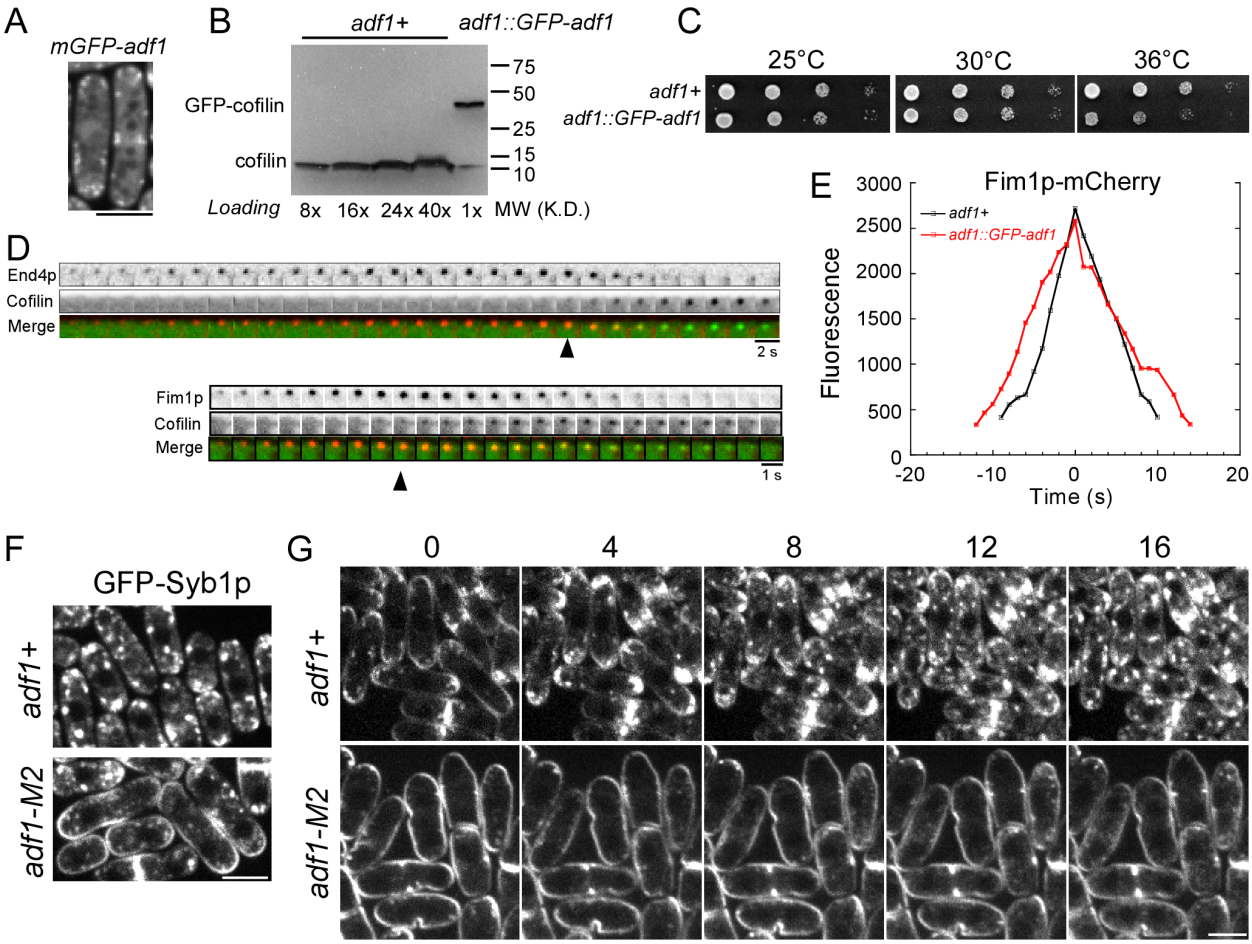

Figure S1: Complementation of *adf1+* deletion by over expression of GFP-Adf1p, related to Figure 1. (A**)** Maximum intensity projection fluorescence micrograph of the full thickness of cells expressing mGFP-Adf1p. **(B)** Western blot with anti-cofilin antibodies to measure the over expression of GFP-Adf1p. The first four lanes from left to right contain whole cell lysates of *adf1*$^{+}$ cells loaded at 8, 16, 24 and 40 times the amount of the lysate of *adf1::Padh-GFP-adf1* cells on the right. Numbers on the right are molecular weight standards in kDa. **(C)** Viability of *adf1*$^{+}$ and *adf1::Padh-GFP-adf1* cells measured by growth of dilution series at 25°C (3 days), 30°C (2 days) or 36°C (2 days). **(D)** Time series of fluorescence micrographs (sums of 3 sections) showing actin patches in cells expressing mGFP-Adf1p and either (upper) End4p-mCherry or (lower) Fim1p-mCherry. mGFP-Adf1p appeared after the actin patches began move (arrowheads) from the cell surface. **(E)** Time courses of the average fluorescence of Fim1p-mCherry in 11 actin patches in *adf1*$^{+}$ (black line and open squares) and *adf1::Padh-GFP-adf1* (red line and filled squares) cells. **(F)** Fluorescence micrographs (middle slice of a fluorescence Z-series) of cells expressing mGFP tagged t-SNARE synaptobrevin, Syb1p: (top) wild type cells; (bottom) *adf1-M2* cells. **(G)** Time course of the uptake of plasma membrane from cells labeled with FM4-64 for 15 min at 4°C and transferred to 25°C for observations. The images are maxim intensity projections of fluorescence micrographs of the 5 middle Z-slices of the cells. Numbers are time in minutes. Bars, 5 µm.

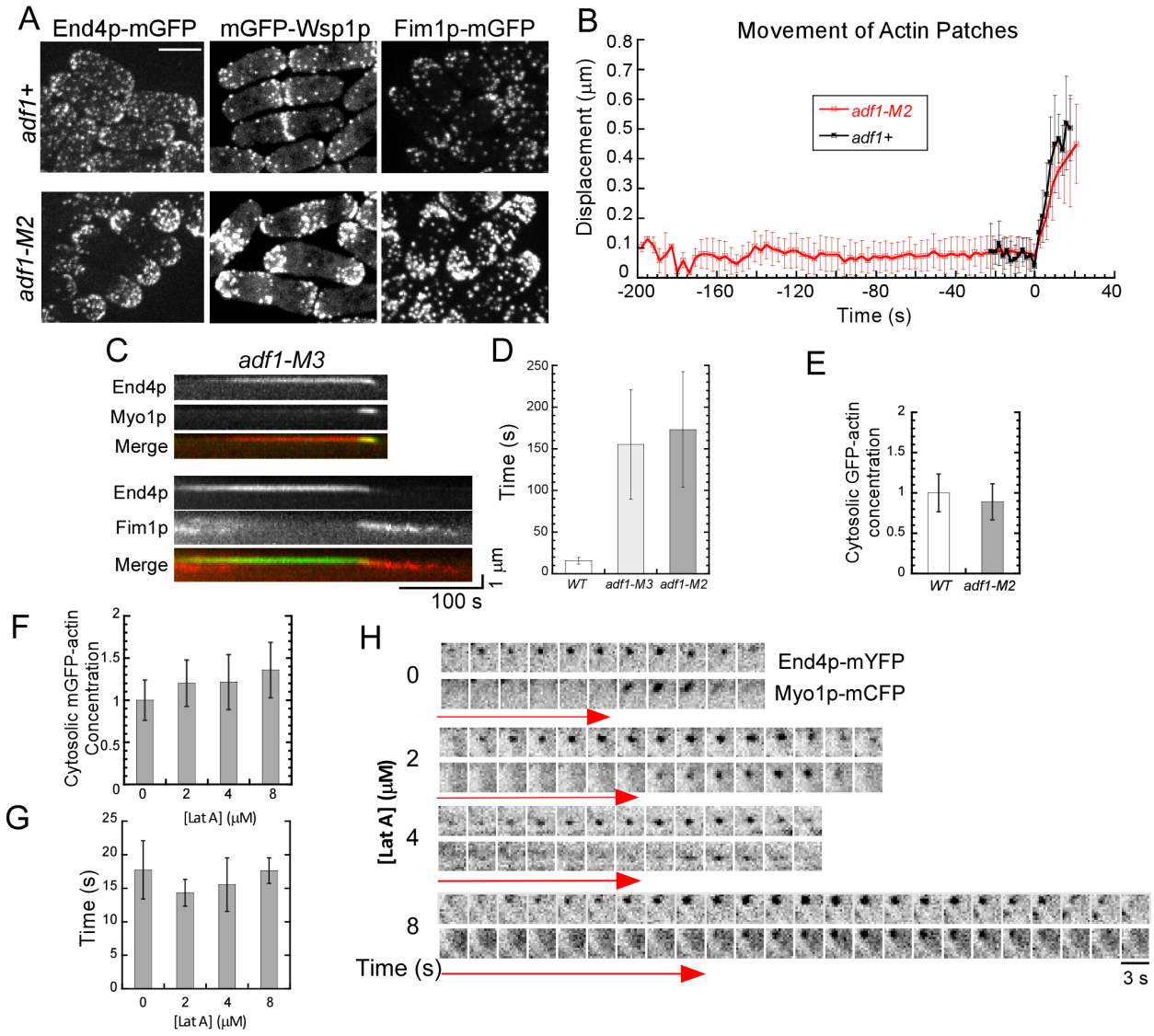

Figure S2: Endocytic defects of cofilin mutant cells, related to Figure 2 and 3. **(A)** Fluorescence micrographs of *adf1+* and *adf1-M2* cells expressing actin patch proteins tagged with mGFP. Micrographs are maxim intensity projections of Z-series images of whole cells. Bar, 5 µm. **(B)** Time course of the displacement of actin patches labeled with mGFP-End4p from the cell surface in wild type cells (black line, filled squares, n = 11 patches) and *adf1-M2* cells (red line, open squares, n = 16 patches). Average distance of patches from the starting position and the standard deviation are shown for each time point. **(C)** Kymographs of actin patches in a*df1-M3* cells expressing both (top) Ent1p-Tdtomato and mGFP-Myo1p or (bottom) End4p-mGFP and Fim1p-mCherry. Both the initiation and disassembly of actin filaments were delayed in the patches of *adf1-M3* cells compared to actin patches in wild type cells (Figure 3D). **(D)** Histogram

shows the average time (± SD) between the appearance of Ent1p-Tdtomato and the appearance of mGFP-Myo1p in actin patches of wild type (n = 20), *adf1-M3* (n = 25) and *adf1-M2* (n = 21) cells. (**E-H)** Comparison of the effects of the *adf1-M2* mutation and Latrunculin A. **(E)** Normalized cytoplasmic mGFP-Act1p concentrations measured by the fluorescence intensity of at least 50 wild type (WT) $adf1^{+}$ and *adf1-M2* cells. **(F)** Histogram of cytoplasmic mGFP-Act1p concentrations in wild type cells treated with LatA for 30 min. **(G)** Histogram of the average time (± SD) between the appearances of End4p and Myo1p in actin patches of cells treated for 30 min with a range of concentrations of LatA. **(H)** Time series fluorescence micrographs at 3 s intervals of actin patches in cells expressing both End4-mYFP and Myo1-mCFP over a range of concentrations of LatA. Each image is the sum of the median 3 slices of the cell. Red arrows indicate the time intervals between recruitment of End4p and Myo1p.

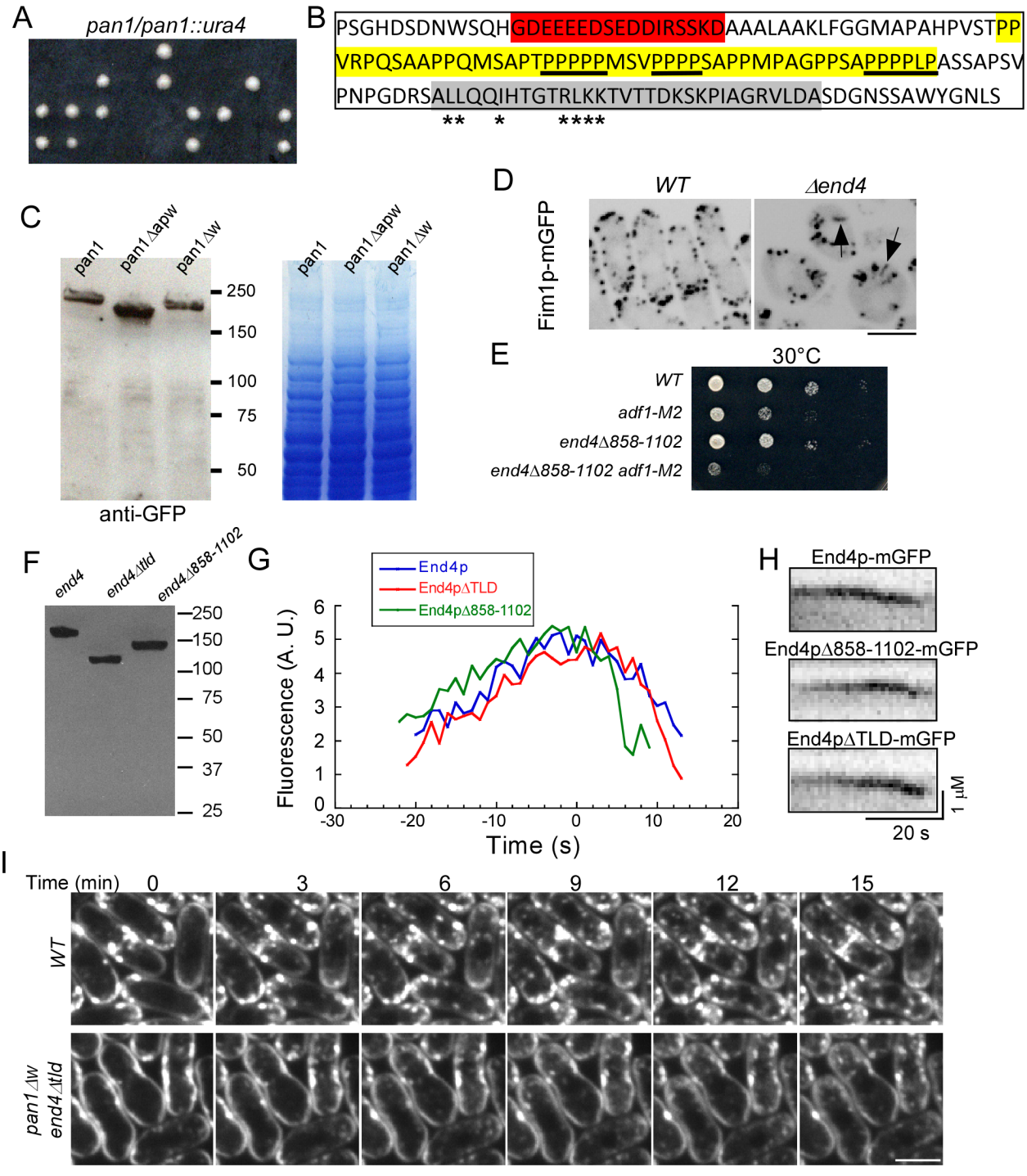
A
pan1/pan1::ura4
B
PSGHDSDNWSQHGDEEEEDSEDDIRSSKDAAALAAKLFGGMAPAHPVSTPP
VRPQSAAPPQMSAPTPPPPPMSVPPPPSAPPMPAGPPSAPPPPLPASSAPSV
PNPGDRSALLQQIHTGTRLKKTVTTDKSKPIAGRVLDASDGNSSAWYGNLS
** * ****
C
pan1
pan1Δapw
pan1Δw
250
150
100
75
50
anti-GFP
D
WT
Δend4
Fim1p-mGFP
E
30°C
WT
adf1-M2
end4Δ858-1102
end4Δ858-1102 adf1-M2
F
end4
end4Δtld
end4Δ858-1102
250
150
100
75
50
37
25
G
End4p
End4pΔTLD
End4pΔ858-1102
Fluorescence (A. U.)
Time (s)
H
End4p-mGFP
End4pΔ858-1102-mGFP
End4pΔTLD-mGFP
1 μM
20 s
I
Time (min)
0
3
6
9
12
15
WT
pan1Δw
end4Δtld

Figure S3: Two adaptor proteins Pan1p and End4p are important for initiating the nucleation of actin in the patches, related to Figure 4 and 5. **(A-C)** Pan1p is essential for endocytosis by fission yeast cells. **(A)** Tetrad dissections of sporulated a *pan1+/pan1::ura+* diploid cells produced two or fewer viable spores, showing the *pan1Δ* cells are not viable. **(B)** Sequence of the C-terminal residues 1643-1799 of fission yeast Pan1p including (red) an acidic motif, (yellow, underlined) 3 polyproline tracts and (gray) a WH2 motif with highly conserved WH2 residues marked with asterisks. **(C)** (Left) Western blot with anti-GFP after SDS-PAGE of lysates of whole cells expressing Pan1p-mGFP, Pan1pΔAPW-mGFP and Pan1pΔW-mGFP cells. Mobilities of molecular weight standards (in kDa) are on the right. (Right) Coomassie blue stain of the gel shows that the equal amounts of each sample of cell lysate were loaded. **(D-H)** The talin-like domains of End4p are not essential for assembly of actin patches. **(D)** Negative contrast fluorescence micrographs of wild type (WT) and *Δend4* cells expressing Fim1-mGFP. Arrows point to elongated actin patches in *Δend4* cells. Images are sums of Z-series of sections of whole cells. **(E)** Viability of strains with one talin-like domain of End4p deleted, *adf-M2* and the double mutants measured by growth of dilution series for 2 days at 30°C. **(F)** Western blot with anti-GFP after SDS-PAGE of the whole cell lysates of equal numbers of *end4-mGFP*, *end4Δ858-1102-mGFP* and *end4Δtld-mGFP* cells. Numbers on the left are molecular weight standards in kDa. **(G)** Time courses of average fluorescence of End4p-mGFP, End4pΔ858-1102-mGFP and End4pΔ663-1102-mGFP in 10 actin patches. **(H)** Kymographs of fluorescence micrographs showing examples of actin patches in cells depending on End4p-mGFP, End4Δ858-1102-mGFP or End4Δ663-1102-mGFP. **(I)** Time course of the uptake of FM4-64 by wild type and *pan1Δw end4Δtld* cells. The images are the sums of fluorescence micrographs of the 5 middle Z-slices of the cells. Numbers are time in min. Bars, 5 μm.

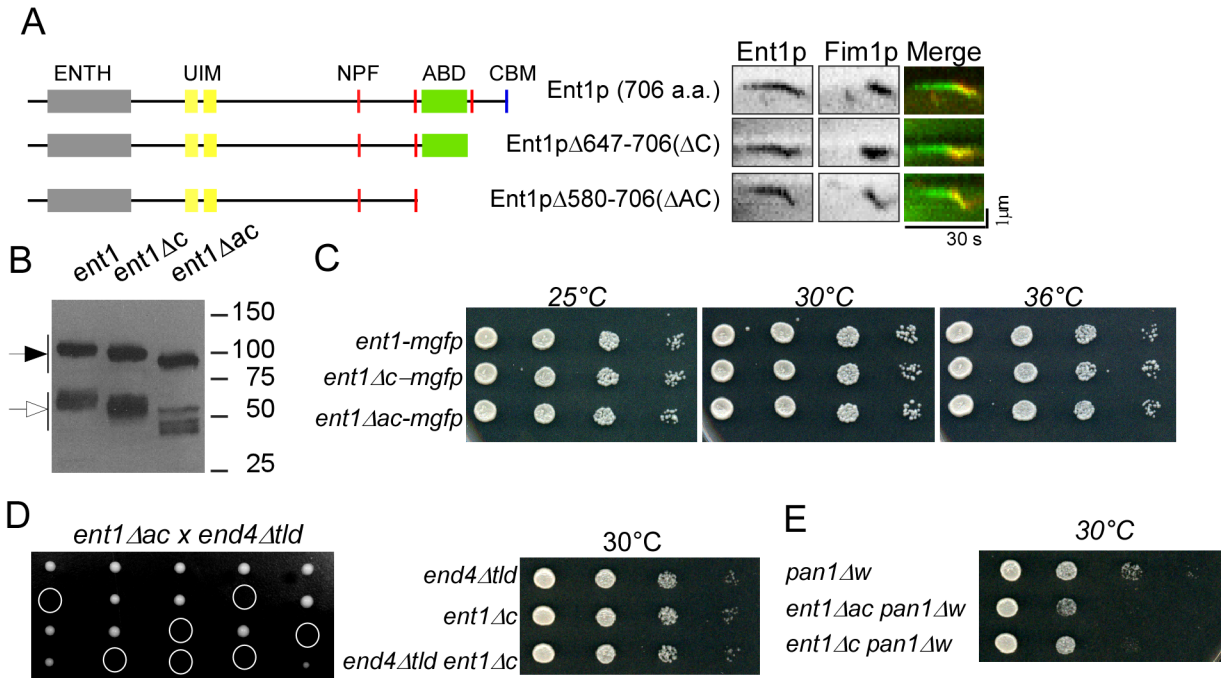

Figure S4: The actin filament binding domain of Ent1p is not required for the assembly of actin patches, related to Figure 5. **(A)** (Left) Domains of full length Ent1p and two truncation mutants. ENTH, Epsin N-terminal homology domain; UIM, ubiquitin interacting motif; NPF, Asn-Pro-Phe motif recognized by EH domains; ABD, actin filament binding motif; and CBM, clathrin binding motif. (Right) Kymographs of fluorescence micrographs of actin patches in cells expressing Fim1p-mCherry (red) and Ent1p or its truncation mutants tagged with mGFP (green). **(B)** Western blot with anti-GFP after SDS-PAGE of lysates of whole cells expressing Ent1p-mGFP, Ent1pΔC-mGFP or Ent1pΔAC-mGFP (arrow). Unfilled arrow points to degradation products of mGFP tagged Ent1p proteins. **(C)** Viability of strains expressing either full length Ent1p or Ent1p truncation mutants measured by growth of dilution series for 4 days at 25°C, 2 days at 30°C or 2 days at 36°C. **(D)** Genetic interactions between *end4Δtld* and either *ent1Δac* or *ent1Δc*. (Left) Growth of tetrad dissections of crosses between *end4Δtld* and *ent1Δac-mGFP*. The double mutant *ent1Δac-mGFP end4Δtld* (circles) was not viable. (Right) Viability of *endΔtld*, *ent1Δc-mGFP* and *endΔtld ent1Δc-mGFP* by growth of dilution series for 2 days at 30°C. **(E)** Viability of *pan1Δw*, *pan1Δw ent1Δac-mGFP* and *pan1Δw ent1Δc-mGFP* by growth of dilution series for 2 days at 30°C.

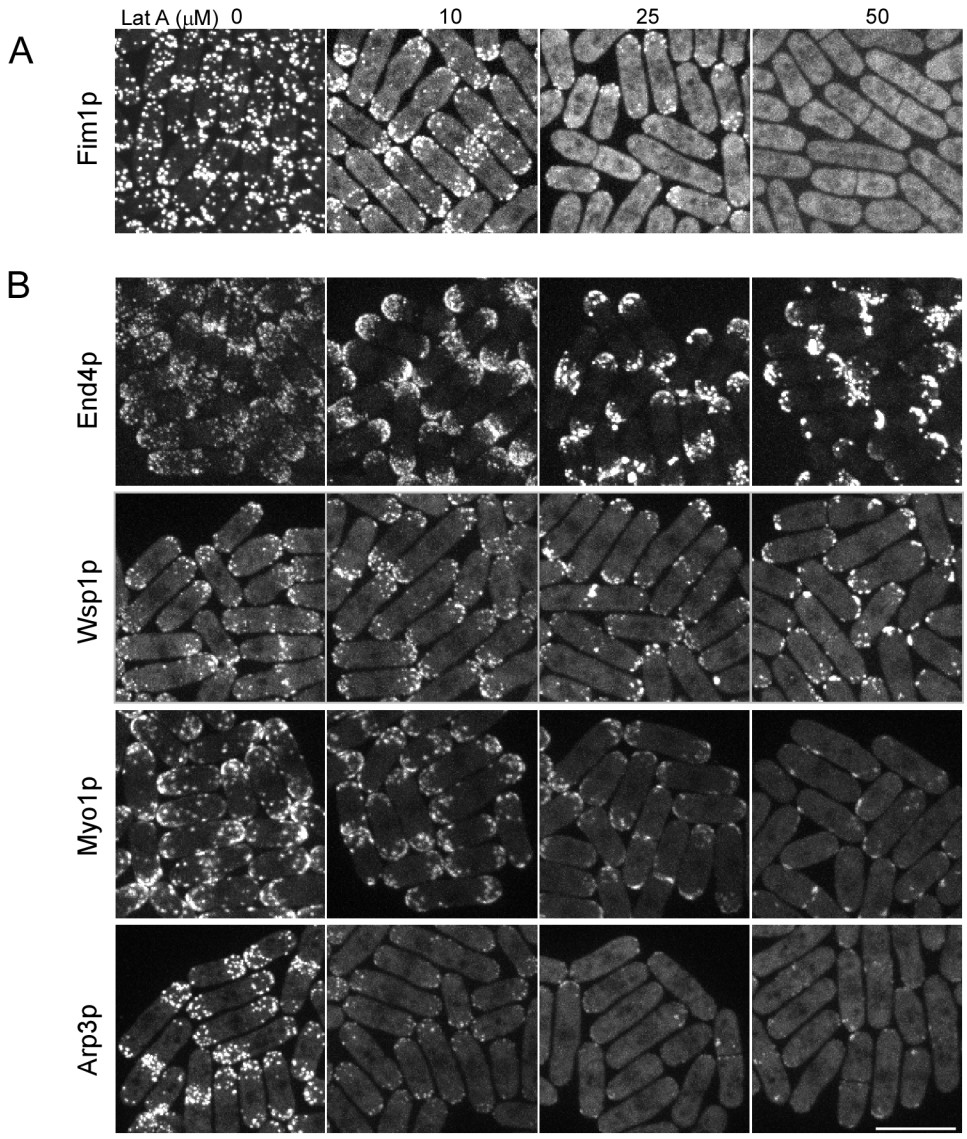

Figure S5: Treatment of cells with a range of high LatA concentrations for 30 min, related to Figure 6. Maximum intensity projections of stacks of fluorescence micrographs of live cells expressing various fluorescence markers. **(A)** Fim1p-mGFP. **(B)** End4p-mGFP, mGFP-Wsp1p, mGFP-Myo1p or Arp3p-mGFP. Bar, 10 μm.

Table S1: List of Strains

Name	Genotype	Source
QC94	*Kan-Padh-mGFP-Adf1 leu1-32 ura4-D18 his3-D1 ade6-M216*	This study
QC332	*Kan-Padh-mGFP-Adf1 fim1-mCherry-NatMX6*	This study
QC336	*Kan-Padh-mGFP-Adf1 end4-mCherry-NatMX6*	This study
QC306	*h+ 41nmt1-GFPactin-leu+ ura4-D18 his3-D1 ade6-M216*	This study
QC150	*h+ adf1M2-KanMX6 41nmt1-mGFPactin-leu+ ura4-D18 his3-D1 ade6-M216*	This study
TP195	*h+ leu1-32 ura4-D18 his3-D1 ade6 kanMX6- Pmyo1-mGFP-myo1*	V. Sirotkin
QC253	*adf1-M2-KanMX6 myo1-mGFP-KanMX6*	This study
TP401	*h+ leu1-32 ura4-D18 his3-D1 ade6-M210 pan1-mGFP-kanMX6*	V. Sirotkin
QC254	*adf1-M2-KanMX6 Pan1-mGFP-KanMX6*	This study
QC181	*h- leu1-32 ura4-D18 ade6-M210 fim1-mGFP-kanMX*	JQ Wu
QC255	*adf1-M2-KanMX6 Fim1-mGFP-KanMX6*	This study
TP398	*h+ leu1-32 ura4-D18 his3-D1 ade6-M210 end4-mGFP-kanMX6*	V. Sirotkin
QC273	*adf1-M2-kanMX end4-mGFP-kanMX6*	This study
TP199	*h+ leu1-32 ura4-D18 his3-D1 ade6 kanMX6- Pwsp1-mGFP-wsp1*	V. Sirotkin
QC271	*adf1-M2-kanMX kanMX6- Pwsp1-mGFP-wsp1*	This study
QC294	*kanMX6-Pmyo1-mCFP-myo1 end4-mYFP-KanMX6*	This study
QC292	*adf1-M2-KanMX6 kanMX6-Pmyo1-mCFP-myo1 end4-mYFP-KanMX6*	This study
QC278	*KanMX6-GFP-syb1*	M. Edamatsu
QC305	*adf1-M2-KanMX KanMX6-GFP-syb1*	This study
QC394	*pan1::pan1Δ1743-1794-natMX6*	This study
QC348	*leu1-32 ura4-D18 his3-D1 ade6-M216 arp3-mGFP-kanMX6*	Lab stocks
QC396	*pan1::pan1Δ1643-1794-natMX6*	This study
QC382	*pan1::pan1Δ1743-1794-mGFP-KanMX6*	This study
QC403	*pan1::pan1Δ1743-1794-natMX6 adf1-M2-KanMX6*	This study
QC400	*pan1::pan1Δ1643-1794-tdTomato-NatMX6 Kanmx6-mGFP-myo1p*	This study
QC412	*Pan1-mCherry-natMX6 KanMX6-Pmyo1-mGFP-Myo1*	This study
QC399	*pan1-mGFP-KanMX6 fim1-mCherry-NatMX6*	This study
QC389	*pan1::pan1Δ1643-1794-GFP-KanMX6 fim1-mcherry-NatMX6*	This study
QC358	*fim1-mCherry-NatMX6 end4::end4Δ663-1102-mGFP-KanMX6*	This study
QC359	*fim1-mCherry-NatMX6 end4::end4Δ858-1102-mGFP-KanMX6*	This study
QC368	*fim1-mCherry-NatMX6 end4-mGFP-KanMX6*	This study
QC341	*end4::end4Δ663-1102-NatMX6*	This study
QC404	*pan1::pan1Δ1743-1794-NatMX6 end4::end4Δ663-1102-NatMX6*	This study
QC414	*ent1-tdtomato-KanMX6 KanMX6-Pmyo1-mGFP-Myo1*	This study
QC419	*end4::end4Δ663-1102-NatMX6 ent1-tdtomato-KanMX6 KanMX6-Pmyo1-mGFP-Myo1*	This study
QC420	*pan1::pan1Δ1743-1794-NatMX6 ent1-tdtomato-KanMX6 KanMX6-Pmyo1-mGFP-Myo1*	This study

QC417	*pan1::pan1Δ1743-1794-NatMX6 end4::end4Δ663-1102-NatMX6 ent1-tdtomato-KanMX6 KanMX6-Pmyo1-mGFP-Myo1*	This study
QC424	*ent1-tdtomato-KanMX6 KanMX6-Pmyo1-mGFP-Myo1 adf1-M2-KanMX6*	This study
QC469	*adf1-M3-kanMX6 fim1-mcherry-NatMX6 end4-mGFP-kanMX6*	This study
QC473	*adf1-M3-kanMX6 kanMX6-mGFP-myo1 ent1-tdtomato-kanMX6*	This study
QC421	*pan1::pan1Δ1743-1794-NatMX6 fim1-mCherry-NatMX6 end4::end4Δ663-1102-mGFP-KanMX6*	This study
QC405	*pan1::pan1Δ1743-1794-NatMX6 kanMX6-Pmyo1-mCFP-myo1 end4-mYFP-KanMX6*	This study
QC362	*end4::ura4+ fim1-mGFP*	This study
QC340	*end4::end4Δ858-1102-mGFP-KanMX6*	This study
QC338	*end4::end4Δ663-1102-mGFP-KanMX6*	This study
QC323	*kanMX6-P41nmt1-mYFP-lifeact ade6-M210 leu1-32 ura4-D22*	JQ. Wu
QC326	*kanMX6-P41nmt1-mYFP-lifeact end4-mCFP*	This study

Supplemental Experimental Procedures

Cell culture: Fission yeast cells were grown with standard protocols at 25°C unless otherwise specified. Cells were pelleted at 3000 rpm for 1 min and washed with EMM5s medium before fluorescence microscopy. Cells with *41nmt1*-mGFP-actin in the *leu1* locus were induced in EMM5s medium for 18 hours to induce expression before fluorescence microscopy.

Microscopy of live cells: Cells were applied to a 25% gelatin pad made with EMM5s and sealed under a cover slip [1]. Cells were imaged with a 100x Plan Apochromat objective lens (NA 1.40) on an Olympus IX-71 microscope with a confocal spinning disk unit (Yokogawa, CSU-X1) and an Electron Multiplying Charge-Coupled Device (EM-CCD) camera (Andor, iXon). Images were processed using Image J (NIH) with freely available plug-ins.

Rhodamine-phalloidin staining: To visualize actin filaments in fixed cells, we used a modification [1] of a published method (Pelham and Chang, 2001). Cells were fixed with 4% formaldehyde for 5 min, washed with PEM buffer (0.1 M NaPIPES pH 6.8, 1 mM EGTA, 1 mM $MgCl_2$), permeabilized with 1% Triton X-100 in PEM for 2 min and washed with PEM buffer before staining with 8 μM rhodamine-phalloidin in PEM buffer (Invitrogen, CA).

Endocytosis assay with FM4-64 dye: Cells were chilled on ice for 30 min before being labeled with 40 μM FM4-64 in YE5S medium on ice for 15 min. Cells were washed twice with cold YE5S medium and transferred to a slide for observations at 25°C by time lapse fluorescence microscopy.

Latrunculin A treatment: Cells grown to OD_{600} between 0.4-0.6 were treated with Latrunculin A (Enzo Life Sciences, NY) in EMM5s medium at 25°C for 30 min before preparation for microscopy in YE5S medium with the same concentration of LatA.

Quantitation of cytoplasmic mGFP-actin: The sum of the fluorescence in 19 Z-sections at 0.36 μm intervals of whole cells expressing mGFP-actin was corrected for exposure time, camera noise and uneven illumination. We measured the cytoplasmic fluorescence intensity of at least 50 cells in small cellular regions without visible actin patches, nuclei or vacuoles.

Protein purification: DNA encoding for amino acid residues 1633-1794 of Pan1p was amplified from yeast genomic DNA by PCR and subcloned into pGEX-6P-1 vector (GE Health Science).

The GST fusion protein was expressed in *E. coli* BL21-CondonPlus RP cells (Stratagene) induced with 0.5 mM IPTG at 25°C overnight. GST-Pan1$_{1633\text{-}1794}$ was purified from a clarified cell lysates by affinity chromatography on glutathione-Sepharose eluted with 100 mM glutathione, gel filtration on a 2.5 x 100 cm column of Sephacryl S200 (GE Health) in 250 mM NaCl, 1 mM EDTA in 10 mM Tris-Cl (pH 8.0) and anion exchange chromatography on a 2.5 x 10 cm column of DEAE Sepharose Fast Flow (GE Health) loaded with protein in 50 mM NaCl in 50 mM Tris-Cl (pH8.0) and eluted with a gradient of 50-500 mM NaCl in 50 mM Tris-Cl (pH 8.0). Purified protein was stored in KMEI buffer (50 mM KCl, 1 mM $MgCl_2$, 1 mM EGTA, 10 mM imidazole, pH 7.0). Actin was purified from acetone powder of flash frozen chicken breast and stored in buffer G (2 mM Tris-Cl, pH 8.0, 0.5 mM ATP, 0.5 mM DTT, 0.1 mM $CaCl_2$, 1 mM NaN_3) at 4°C [2] .

Western blot of whole cell lysates of yeast cells: Cells from a 10 ml exponentially growing culture in YE5S medium were pelleted, washed and re-suspended in 300 µl of yeast lysis buffer (50 mM Tris-Cl pH 8.0, 100 mM KCl, 3 mM $MgCl_2$, 1 mM EGTA, 0.1% Triton X-100, 1 mM DTT, 1 mM PMSF) and lysed with glass beads in a FastPrep-24 bead beater (MP Biomedicals). The whole cell lysate was boiled for 5 min in Laemmli sample buffer before being analyzed by SDS-PAGE, blotting with anti-GFP antibodies (ab290, ABCAM), and detection with an ECL detection kit (GE Healthcare).

Binding GST-Pan1$_{1633\text{-}1794}$ to actin filaments: Ca-ATP-actin monomers were converted to Mg-ATP-actin monomers by adding to buffer G EGTA to 1 mM and $MgCl_2$ to 0.1 mM for 2 min at 25° C and then polymerized in KMEI buffer at room temperature for 1 h. GST-Pan1$_{1633\text{-}1794}$ was incubated with a range of actin filament concentrations at room temperature in KMEI buffer for 30 min and then centrifuged at 55,000 rpm for 40 min at 4 °C in a TLA100 rotor (average force 212,300 g) in an Ultima TLX ultracentrifuge (Beckman Coulter). Samples of the supernatants were analyzed by SDS-PAGE, staining with Coomassie blue and densitometry.

Estimation of the diffusion coefficient of short actin fragments: The translational diffusion coefficient (D) of actin filaments was calculated based on the following equation [50]:

$$D = \left(\frac{kT}{3\pi\theta L}\right)\left(\ln\left(\frac{2L}{d}\right) - \left(\frac{1}{2}\right)\left(1.46 - 7.4\left(\frac{1}{\ln\left(\frac{2L}{d}\right)} - 0.34\right)^2 - 4.2\left(\frac{1}{\ln\left(\frac{2L}{d}\right)} - 0.39\right)^2\right)\right)$$

k is the Boltzmann constant, $T = 298°$ K is the absolute temperature, $\theta = 2.0$ centipoise [51] is the viscosity of cytoplasm, $L = 81$ nm is the length of an actin filament with 30 subunits and $d = 7$ nm is the diameter of an actin filament.

Supplemental Results

We tested whether a recently identified actin filament binding motif (ABD) in the fission yeast homologue of Epsin (Ent1p) [3] might play a role in initiating actin assembly in patches. Like its budding yeast homologs [4], Ent1p also has an Asn-Pro-Phe (NPF) motif and a clathrin binding motif near the C-terminus (Fig. S4A). We made two truncation mutants of Ent1p, *ent1*Δ*647-706* (*ent1*Δ*c)* lacking the C-terminal sequence and *ent1*Δ*580-706 (ent1*Δ*ac)* lacking the actin filament binding motif and C-terminal sequence, both tagged with mGFP at their C-termini and expressed at a similar level as the full length protein (Figure S4A and B). Neither mutation affected growth (Figure S4C) or the assembly of actin patches compared with cells depending on full length Ent1p-mGFP (Figure S4A).

The *end4*Δ*tld* mutation was synthetic lethal with the *ent1*Δ*ac* mutation ((Figure S4D and E), but not the shorter *ent1*Δ*c* truncation mutation retaining the ABD (Figure S4D). The lethality of the double mutant prevented us from determining whether there is a delay in the nucleation of actin filament network at actin patches in these cells. Therefore, the actin filament binding motifs of End4p and Ent1p may have redundant functions, so the absence of both motifs is lethal.

Neither the *ent1*Δ*ac* nor the *ent1*Δ*c* mutations showed genetic interactions with *pan1Δw* (Figure S4E). Further, the delay in the initiation of actin filament nucleation in the patches of double mutant *pan1Δw ent1Δac* cells (56 ± 21 s, n = 18) was the same as that in *pan1Δw* cells. Thus, the functions of the actin filament binding motif of Ent1p do not overlap with those of Pan1p.

We attempted to image small actin filaments diffusing from patches in cells expressing both mGFP-LifeAct (to tag filaments) and End4p-Tdtomato (to label early endocytic pits). We observed the structures known to contain actin filaments, actin patches, interphase cables and contractile rings, but we did not detect mGFP over the high cytoplasmic background in nascent actin patches before the burst of actin polymerization at time zero (data not shown). Given the signal to noise we estimate the number of actin molecules associated with early actin patches is <5% the peak numbers of about 7000 actin molecules. We note that single filaments suffice to initiate branching nucleation [5].

We treated wild type cells with a range of concentrations LatA to determine the role of actin filaments in recruiting actin patch proteins. LatA at 50 μM blocked actin polymerization

judging from the lack of Fim1p-mGFP in actin patches (Figure S5A). Recruitment of Arp2/3 complex to actin patches was even more sensitive to LatA (Figure S5B). In contrast, even 50 μM LatA did not prevent recruitment of the adaptor protein End4p to endocytic patches, although those patches became aggregated together in the presence of LatA (Figure S5B). Recruitment of Myo1p to patches was more sensitive to LatA than Wsp1p, which aggregated in punctate structures at the poles of cells like End4p (Figure S5B). Therefore, in the absence of actin filaments End4p and Wsp1p accumulated in patches that did not recruit Myo1p or Arp2/3 complex.

Supplemental References

1. Chen, Q., and Pollard, T.D. (2011). Actin filament severing by cofilin is more important for assembly than constriction of the cytokinetic contractile ring. J Cell Biol *195*, 485-498.
2. MacLean-Fletcher, S., and Pollard, T.D. (1980). Identification of a factor in conventional muscle actin preparations which inhibits actin filament self-association. Biochem Biophys Res Commun *96*, 18-27.
3. Skruzny, M., Brach, T., Ciuffa, R., Rybina, S., Wachsmuth, M., and Kaksonen, M. (2012). Molecular basis for coupling the plasma membrane to the actin cytoskeleton during clathrin-mediated endocytosis. Proc Natl Acad Sci U S A.
4. Wendland, B., Steece, K.E., and Emr, S.D. (1999). Yeast epsins contain an essential N-terminal ENTH domain, bind clathrin and are required for endocytosis. EMBO J *18*, 4383-4393.
5. Achard, V., Martiel, J.L., Michelot, A., Guerin, C., Reymann, A.C., Blanchoin, L., and Boujemaa-Paterski, R. (2010). A "primer"-based mechanism underlies branched actin filament network formation and motility. Curr Biol *20*, 423-428.